MOLECULAR AND CELLULAR BIOLOGY, Mar. 2011, p. 1174–1185 Vol. 31, No. 6
0270-7306/11/$12.00 doi:10.1128/MCB.00903-10

Neuropilin-1 Signaling through p130^{Cas} Tyrosine Phosphorylation Is Essential for Growth Factor-Dependent Migration of Glioma and Endothelial Cells$^{\nabla}$

Ian M. Evans,[1] Maiko Yamaji,[1]† Gary Britton,[1]† Caroline Pellet-Many,[1] Claire Lockie,[1,2] Ian C. Zachary,[1]‡* and Paul Frankel[1,2]‡*

Centre for Cardiovascular Biology and Medicine, Division of Medicine,[1] and Ark Therapeutics Limited,[2] The Rayne Building, University College London, London WC1E 6JJ, United Kingdom

Received 5 August 2010/Returned for modification 6 September 2010/Accepted 28 December 2010

Neuropilin-1 (NRP1) is a receptor for vascular endothelial growth factor (VEGF) and plays an important role in mediating cell motility. However, the NRP1 signaling pathways important for cell motility are poorly understood. Here we report that p130^{Cas} tyrosine phosphorylation is stimulated by hepatocyte growth factor and platelet-derived growth factor in U87MG glioma cells and VEGF in endothelial cells and is dependent on NRP1 via its intracellular domain. In endothelial cells, NRP1 silencing reduced, but did not prevent, VEGF receptor 2 (VEGFR2) phosphorylation, while expression of a mutant form of NRP1 lacking the intracellular domain (NRP1ΔC) did not affect receptor phosphorylation in U87MG cells or human umbilical vein endothelial cells (HUVECs). In HUVECs, NRP1 was also required for VEGF-induced phosphorylation of proline-rich tyrosine kinase 2, which was necessary for p130^{Cas} phosphorylation. Importantly, knockdown of NRP1 or p130^{Cas} or expression of either NRP1ΔC or a non-tyrosine-phosphorylatable substrate domain mutant protein (p130^{Cas15F}) was sufficient to inhibit growth factor-mediated migration of glioma and endothelial cells. These data demonstrate for the first time the importance of the NRP1 intracellular domain in mediating a specific signaling pathway downstream of several receptor tyrosine kinases and identify a critical role for a novel NRP1-p130^{Cas} pathway in the regulation of chemotaxis.

Neuropilin-1 (NRP1) is a coreceptor for vascular endothelial growth factor (VEGF) in endothelial cells and is essential for embryonic angiogenesis and vascular development (10, 29). Though the precise cellular functions of NRP1 have yet to be elucidated, there is a growing body of evidence supporting a key role for NRP1 in the migration of both endothelial and tumor cells (9, 11, 15, 19). NRP1 is thought to act as a coreceptor for VEGF by forming complexes with the VEGF receptor tyrosine kinase (RTK) VEGFR2. Complexation between NRP1 and VEGFR2 enhances VEGF binding, and inhibition of complex formation is associated with reduced VEGFR2 phosphorylation, intracellular signaling, mitogenesis, cell migration, and angiogenesis (16, 18, 28, 34, 35). However, the precise role of NRP1 in VEGF signaling remains unclear. Recent evidence indicates that NRP1 also regulates tumor and vascular cell functions stimulated by other growth factors, such as hepatocyte growth factor (HGF) and platelet-derived growth factor (PDGF). Overexpression of NRP1 promotes tumor progression by potentiating the effect of the HGF/c-Met pathway, and tumor cell invasion mediated by the HGF/c-Met pathway is dependent on NRP1 through an association with c-Met (11, 15). Furthermore, NRP1 and NRP2 can bind HGF and mediate HGF stimulation of endothelial cell migration and proliferation (30). A recent report showed that NRP1 is also required for tumor cell-derived PDGF-mediated migration of smooth muscle cells (2). While these results indicate that NRP1 is required for optimal growth factor signaling important for cell motility, it remains unclear whether NRP1 is critical for specific signaling events induced by growth factors and what those key NRP1-mediated signaling events are.

The 44-amino-acid intracellular domain of NRP1 lacks a defined signaling function but contains the carboxy-terminal consensus PDZ (postsynaptic density 95, disk large, zona occludens 1) domain binding motif SEA, which associates with the PDZ domain protein synectin, also called neuropilin-interacting protein 1 (NIP-1), or RGS-GAIP-interacting protein 1 (GIPC1) (3). The NRP1 intracellular domain, through its association with synectin, has been implicated in NRP1-mediated migration, VEGF-mediated vesicular trafficking, and NRP1/VEGFR2 complex formation (20, 25, 34). Furthermore, expression of an NRP1 mutant form lacking the C-terminal SEA residues or knockdown of synectin disrupted vessel formation in zebrafish embryos, phenocopying the effects of NRP1 knockdown (33).

Recently, we reported that NRP1 is modified by the addition of chondroitin sulfate and that overexpression of a nonmodifiable mutant (S612A) form of NRP1 leads to increased invasion of U87MG glioma cells, which is dependent on the adapter protein p130^{Cas} (9). Here, we investi-

* Corresponding author. Mailing address for Ian C. Zachary: UCL Division of Medicine, 5 University Street, London WC1E 6JJ, United Kingdom. Phone: 44 (0) 207 679 6620. Fax: 44 (0) 207 679 6212. E-mail: I.Zachary@ucl.ac.uk. Mailing address for Paul Frankel: UCL Division of Medicine, 5 University Street, London WC1E 6JJ, United Kingdom. Phone: 44 (0) 207 679 6603. Fax: 44 (0) 207 679 6379. E-mail: p.frankel@ucl.ac.uk.

† These authors contributed equally to this work.

‡ These authors contributed equally to this work.

$^{\nabla}$ Published ahead of print on 18 January 2011.

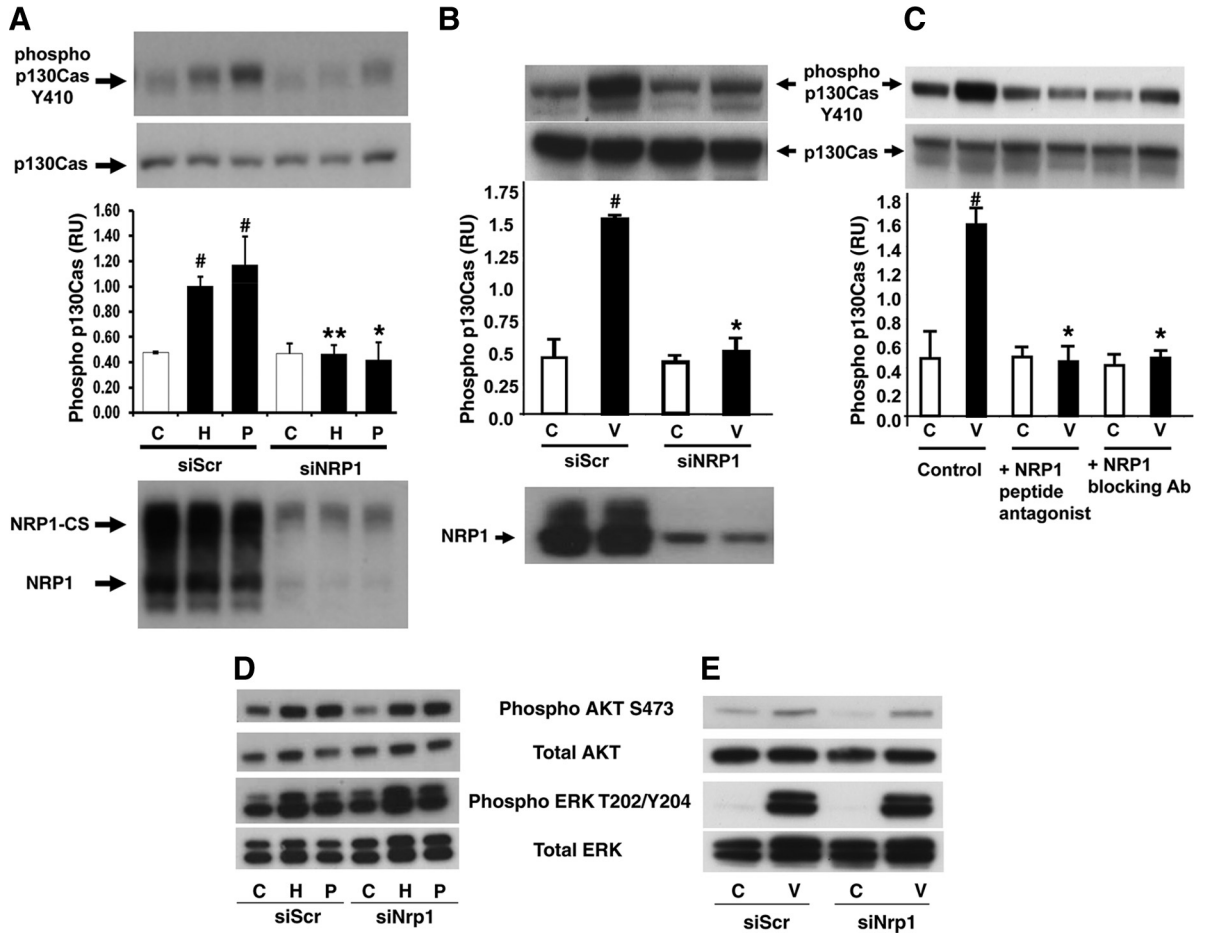

FIG. 1. Growth factor-stimulated tyrosine phosphorylation of p130^{Cas} is mediated via NRP1 in glioma and endothelial cells. (A) U87MG cells were transfected with 25 nM siRNA targeting NRP1 (siNRP1) or 25 nM control scrambled siRNA (siScr). At 48 h posttransfection, cells were incubated in serum-free medium (SFM) for ~18 h prior to treatment with the SFM vehicle control (C) or treated with 25 ng/ml HGF (H) or 50 ng/ml PDGF-BB (P) for 5 min. Cell lysates were then prepared, blotted, and probed with the indicated antibodies. The positions of chondroitin sulfate-glycosylated NRP1 (NRP1-CS; 250 kDa) and unmodified NRP1 (130 kDa) in U87MG cells are indicated. (B) HUVECs were transfected with 200 nM siNRP1 or 200 nM siScr. At 48 h after transfection, cells were switched to EBM containing 0.5% (vol/vol) serum and incubated overnight. Cells were then treated for 10 min with the SFM vehicle control (C) or with 25 ng/ml VEGF-A (V). Cell lysates were then prepared, blotted, and probed with the indicated antibodies. (C) Confluent HUVECs were preincubated for 30 min with SFM plus 100 μM EG0086 (peptide antagonist), 5 μg/ml NRP1 blocking antibody (Ab), or the vehicle (control) and then stimulated with 25 ng/ml VEGF-A (V) or with no further treatment (C) for 10 min. Cell lysates were then prepared, blotted, and probed with the indicated antibodies. (D and E) U87MG cells and HUVECs were treated as described for panels A and B and probed with the indicated antibodies. The blots shown here and in all subsequent figures are representative of at least three separate experiments. In panels A, B, and C, quantitation of p130^{Cas} phosphorylation was performed by densitometry using ImageJ. In each panel, data from three independent experiments are presented as relative units (RU) of p130^{Cas} phosphorylation (means ± SEM) normalized to total p130^{Cas}. *, $P < 0.05$; **, $P < 0.01$ (compared to ligand-stimulated siScr or the control); #, $P < 0.05$ (compared to the control [C]).

gated the role of NRP1 in p130^{Cas} signaling in chemotactic responses to growth factors. We show that NRP1 is essential for tyrosine phosphorylation of p130^{Cas} in response to HGF and PDGF in U87MG glioma cells and VEGF in endothelial cells. In addition, expression of an NRP1 mutant form lacking the intracellular domain (NRP1ΔC) indicated that this domain is crucial for NRP1-mediated RTK signaling. Furthermore, knockdown of either NRP1 or p130^{Cas} or expression of NRP1ΔC or a mutant form of p130^{Cas} deficient in all 15 tyrosines of the "YXXP" motif within the substrate domain (SD) (p130^{Cas15F}) inhibited the growth factor-mediated migration of glioma and endothelial cells. These results indicate that NRP1 plays a central role in growth factor signaling via p130^{Cas}, thus identifying a novel mechanism regulating cell motility.

MATERIALS AND METHODS

Cell culture. U87MG cells (a kind gift of P. Parker) were cultured in Dulbecco's modified Eagle's medium (DMEM) containing 10% (vol/vol) fetal calf serum (FCS) supplemented with penicillin-streptomycin (1:100; P4333; Sigma). Human umbilical vein endothelial cells (HUVECs) were purchased from TCS CellWorks (Buckingham, United Kingdom) and cultured in endothelial basal medium (EBM; Cambrex BioScience Ltd., Nottingham, United Kingdom) supplemented with gentamicin-ampicillin, epidermal growth factor (EGF), bovine brain extract (Singlequots; Cambrex), and 10% FCS. HUVECs used in experiments were no more than passage 6.

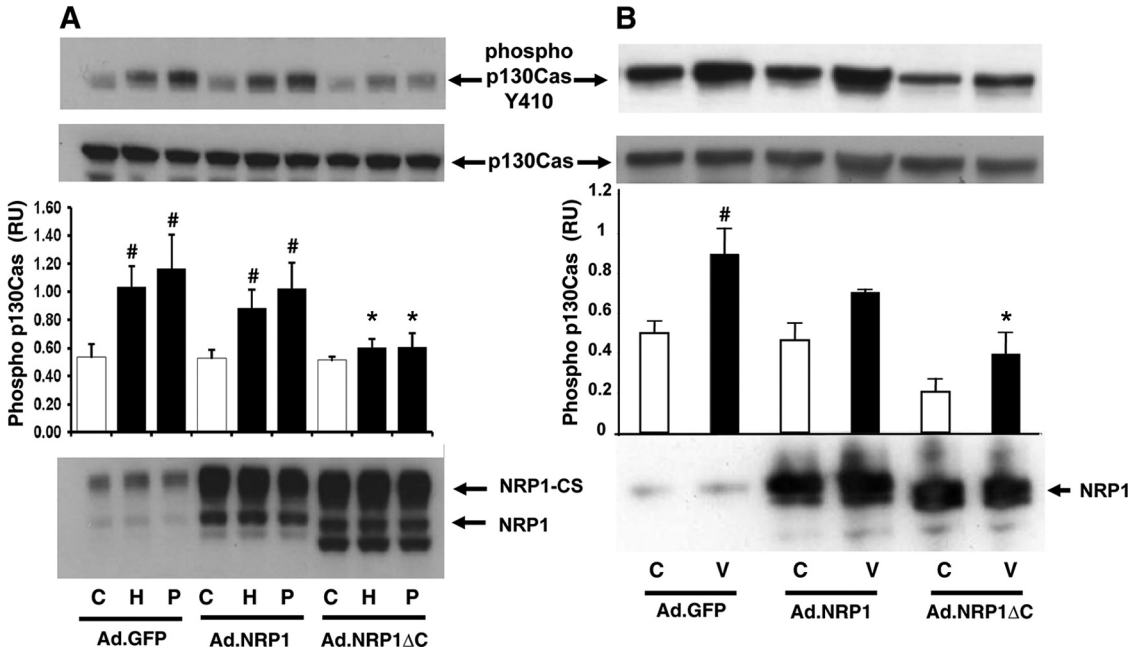

FIG. 2. The NRP1 intracellular domain is required for growth factor-stimulated tyrosine phosphorylation of $p130^{Cas}$. (A) U87MG cells (~80% confluent) were infected with Ad.GFP, Ad.NRP1, or Ad.NRP1ΔC at an MOI of 10. At 48 h after infection, cells were incubated in SFM for ~18 h prior to treatment with HGF and PDGF as described in the legend to Fig. 1. (B) Confluent HUVECs were infected as detailed for panel A, and 48 h after infection, cells were switched to EBM containing 0.5% (vol/vol) serum and incubated overnight. HUVECs were treated with SFM vehicle control (C) or with 25 ng/ml VEGF-A (V). Cell lysates were then prepared, blotted, and probed with the indicated antibodies, and $p130^{Cas}$ phosphorylation was quantified. *, $P < 0.05$ (compared to Ad.GFP plus VEGF, HGF, or PDGF); #, $P < 0.05$ (compared to the control [C]).

Antibodies, reagents, and small interfering RNAs (siRNAs). Antibodies to the NRP1 carboxy terminus (C-19), glyceraldehyde 3-phosphate dehydrogenase (GAPDH; V-18), and synectin (C-20) were from Santa Cruz Inc. (Heidelberg, Germany). NRP1 blocking antibody (catalog no. AF566) and NRP1 extracellular domain antibody (catalog no. AF3870) were from R&D Systems (Abingdon, United Kingdom). Proline-rich tyrosine kinase 2 (PYK2), phospho-PYK2 (Y402), ERK, phospho-ERK (T202/Y204), AKT, phospho-AKT (S473), and phospho-$p130^{Cas}$ (Y410) antibodies were from Cell Signaling Technology Inc. (Danvers, MA). $p130^{Cas}$ monoclonal antibody was from BD Transduction Labs (Oxford, United Kingdom). Alexa Fluor 486–donkey anti-goat antibody, Alexa Fluor 546–donkey anti-rabbit antibody, and Alexa Fluor 555-phalloidin were from Invitrogen (Paisley, United Kingdom). EG00086 was designed and synthesized as described previously (13) and by Bachem Inc. (Weil am Rhein, Germany) with >90% purity. Full details of the biological characterization of EG00086 are described elsewhere (13). PF573228 was purchased from Tocris Bioscience (Bristol, United Kingdom). Recombinant HGF, PDGF-BB, and VEGF-A165 were from R&D Systems (Abingdon, United Kingdom). Control siRNA 1 (catalog no. AM4635) was purchased from Applied Biosystems (Warrington, United Kingdom). Target sequences for siRNAs were as follows: NRP1 siRNA, 5′-GGAUUUUCCAUACGUUAUtt-3′; $p130^{Cas}$ siRNA, 5′-GGUCGACAGUGGUGUGUAUtt-3′; $p130^{Cas}$#2 siRNA, 5′-GGAUGGAGGACUAUGACUAtt-3′; PYK2 siRNA, 5′-CAGGAGAACUUAAAGCCCAtt-3′; synectin (GIPC1) siRNA, 5′-AGGACAAAAGGAACCCGGtt-3′; FAK siRNA, 5′-GAUGUUGGUUUAAAGCGAUtt-3′.

siRNA transfection. U87MG cells at 60% confluence were transfected with Lipofectamine 2000 (Invitrogen) using a 25 nM final concentration of siRNA. HUVECs at ~70% confluence were transfected with Oligofectamine Reagent (Invitrogen) and 200 nM siRNA as described previously (8).

Ad construction and infection. NRP1ΔC cDNA was generated from wild-type (WT) NRP1 by the insertion of a stop codon (TAC to TAG) after the transmembrane region (amino acid residue 880) using the QuikChange mutagenesis kit (Stratagene, Cheshire, United Kingdom). $p130^{Cas15F}$ cDNA was generated from $p130^{Cas}$ by mutating all 15 tyrosines within the consensus motif YXXP of the SD of $p130^{Cas}$ to phenylalanine. Adenoviruses (Ad) expressing NRP1, NRP1ΔC, $p130^{Cas}$, and $p130^{Cas15F}$ were generated using the GATEWAY vector (pAd/CMV/V5-DEST; Invitrogen), and Ad were produced by transfection into host HEK293A cells (Invitrogen). The viral particles were purified by cesium chloride centrifugation, virus titers were determined by immunoassay (QuickTiter Adenovirus Titer Immunoassay kit; Cell Biolabs, San Diego, CA), and Ad were stored at −20°C. U87MG cells or HUVECs were infected with Ad expressing either green fluorescent protein (Ad.GFP), NRP1 (Ad.NRP1), or NRP1ΔC (Ad.NRP1ΔC) at a multiplicity of infection (MOI) of 10. U87MG cells or HUVECs were infected with Ad expressing either LacZ (Ad.LacZ), $p130^{Cas}$ (Ad.$p130^{Cas}$), or $p130^{Cas15F}$ (Ad.$p130^{Cas15F}$) at an MOI of 250.

Immunoblotting and enzyme-linked immunosorbent assay (ELISA). For immunoblotting, cells were lysed in a solution containing 50 mM Tris-HCl (pH 7.5), 1% Triton X-100, 150 mM NaCl, 5 mM EDTA, complete protease inhibitor (Roche), and phosphatase inhibitors I and II (Sigma) and analyzed by sodium dodecyl sulfate-polyacrylamide gel electrophoresis using 4 to 12% Bis-Tris gels (NuPAGE; Invitrogen), followed by electrotransfer onto Invitrolon polyvinylidene difluoride membranes (Invitrogen). Membranes were blocked with 5% (wt/vol) nonfat dry milk and 0.1% (vol/vol) Tween 20 in Tris-buffered saline for 1 h at room temperature before being probed with the primary antibody by overnight incubation at 4°C, followed by incubation for 1 h at room temperature with a horseradish peroxidase-linked secondary antibody (Santa Cruz) and detection using ECL plus reagents (GE Healthcare, Little Chalfont, United Kingdom) in accordance with the manufacturer's protocol. Immunoblots were quantified by scanning films with a calibration strip and analyzed by densitometry using ImageJ (U.S. National Institutes of Health; http://rsb.info.nih.gov/ij/). ELISA kits for measurement of total PDGFRβ (catalog no. DYC385-2), total phosphotyrosine PDGFRβ (catalog no. DYC1767-2), total VEGFR2 (catalog no. 7340), and VEGFR2 phosphotyrosine 1175 (catalog no. 7335) were purchased from R&D Systems, and assays were performed in accordance with the manufacturer's protocol.

Immunofluorescence and confocal imaging. For immunofluorescent staining, cells were fixed in 100% methanol (−20°C) for 2 min and then rehydrated in phosphate-buffered saline (PBS) for 30 min. Antibody incubations were performed overnight at 4°C in 1% (wt/vol) bovine serum albumin–0.1% (vol/vol) Tween 20 in PBS. Confocal imaging was performed using a Leica SPE2 upright microscope running Leica LAS software using sequential imaging capture (Leica Microsystems, Milton Keynes, United Kingdom). Colocalization was quantified using Volocity 4.1 imaging software (Improvision, Perkin-Elmer, Cambridge, United Kingdom). Images were processed so that voxels with identical *x* and *y*

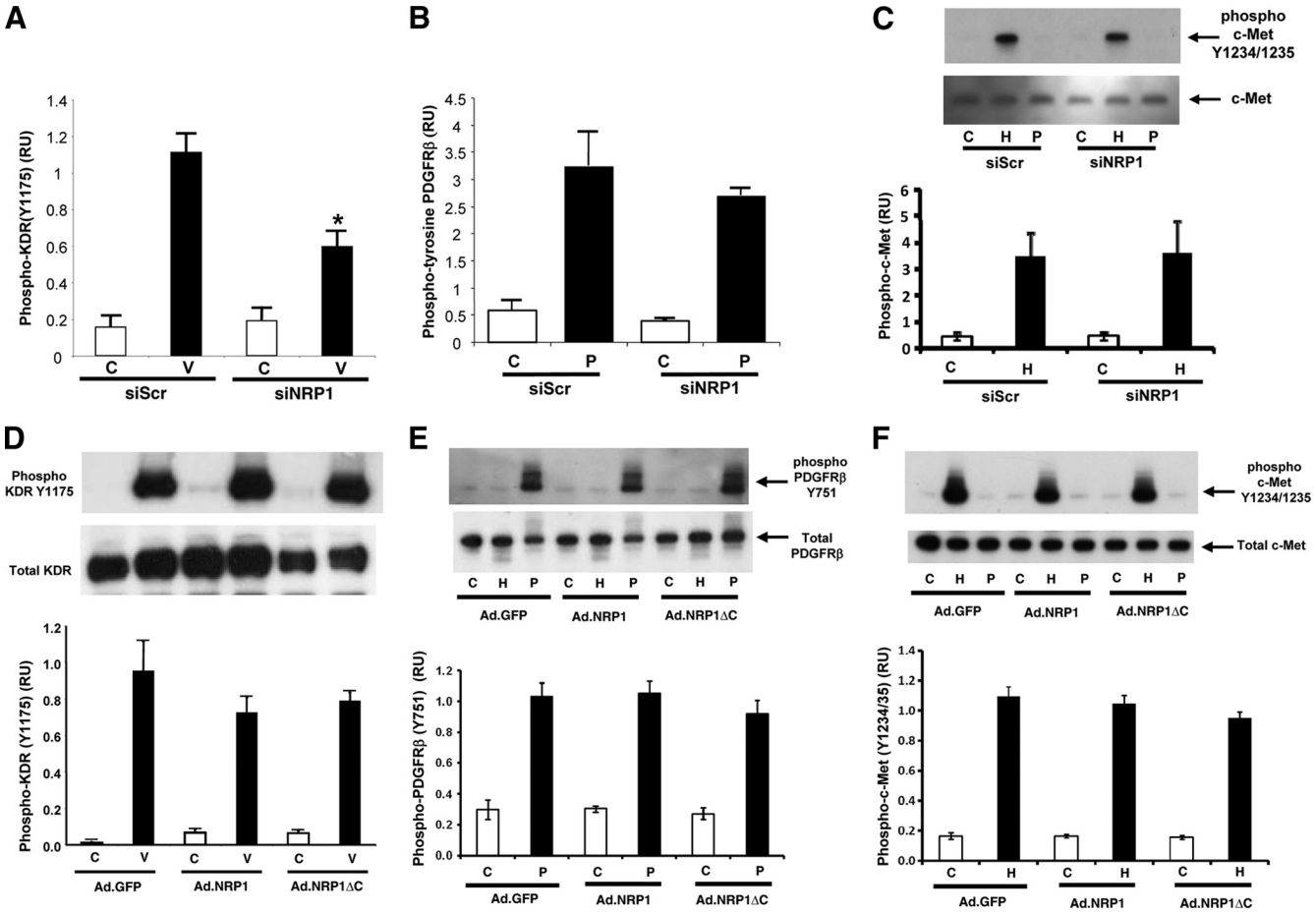

FIG. 3. The cytosolic domain of NRP1 is not required for RTK phosphorylation. (A) HUVECs were transfected and treated as described in the legend to Fig. 1B. Cell lysates were then prepared, and total VEGFR2 and phospho-VEGFR2 (pY1175) levels were measured by ELISA. (B) U87MG cells were transfected and treated with PDGF-BB as described in the legend to Fig. 1A. Cell lysates were prepared, and total PDGFRβ and phospho-PDGFRβ (total tyrosine) levels were measured by ELISA. For panels A and B, data from three independent experiments are presented as relative phosphorylation units (RU) (means ± SEM) normalized to the total receptor level. *, $P < 0.05$ (compared with VEGF-treated siScr). (C) U87MG cells were transfected and treated with HGF as described in the legend to Fig. 1A. Cell lysates were then prepared, blotted, and probed with the antibodies for total c-Met and phospho-c-Met (Tyr1234/1235). (D, E, and F) Cell lysates from Fig. 2A and B were prepared, blotted, and probed with the indicated antibodies. Phosphorylation was quantified as described in the legend to Fig. 1. There were no significant differences in growth factor-stimulated receptor phosphorylation between any of the virus treatments in each panel.

coordinates from both the NRP1 channel and the phospho-p130Cas channel were considered to be colocalized.

Transwell chemotactic migration assay. Transwell cell culture inserts made of transparent, low-pore-density polyethylene terephthalate with an 8-μm pore size (Falcon; BD Biosciences, Oxford, United Kingdom) were inserted into a 24-well plate. Serum-free medium (SFM) with or without the indicated growth factors or the vehicle was placed in the bottom chamber, and cells in suspension (1.5×10^5/well in serum-free EBM or serum-free DMEM for HUVECs and U87MG, respectively) were added to the top chamber and incubated at 37°C for 4 h (HUVECs) or 6 h (U87MG). Cells that had not migrated or had only adhered to the upper side of the membrane were removed before the membrane was fixed and stained with a Reastain Quik-Diff kit (IBG Immucor Ltd., West Sussex, United Kingdom) using the manufacturer's protocol and mounted on a glass slide. Cells that had migrated to the lower side of the membrane were counted in four random fields per well at ×20 magnification using an indexed eyepiece graticule.

Statistical analysis. The data displayed on the graphs are means, with error bars representing the standard error of the mean (SEM). Statistical analysis was performed by two-way analysis of variance with a Bonferroni posttest. A P value of <0.05 was considered significant.

RESULTS AND DISCUSSION

Tyrosine phosphorylation of p130Cas is known to play an important role in cell motility (5), but relatively little is known about the extracellular factors and receptors which mediate this pathway or the mechanisms involved (1, 7, 22). We recently showed that NRP1 overexpression leads to an increase in tyrosine phosphorylation of p130Cas, which was required for cell motility (9), raising the possibility that NRP1 could be an important endogenous mediator of p130Cas signaling in cell migration. This was examined by testing the effects of three potent chemotactic factors on the levels of tyrosine-phosphorylated p130Cas in endothelial and tumor cells. Treatment of U87MG cells with HGF (25 ng/ml) or PDGF (50 ng/ml) or of HUVECs with VEGF (25 ng/ml) strongly increased p130Cas tyrosine phosphorylation, which was markedly reduced when cells were treated with siRNA to NRP1 (Fig. 1A and B). In

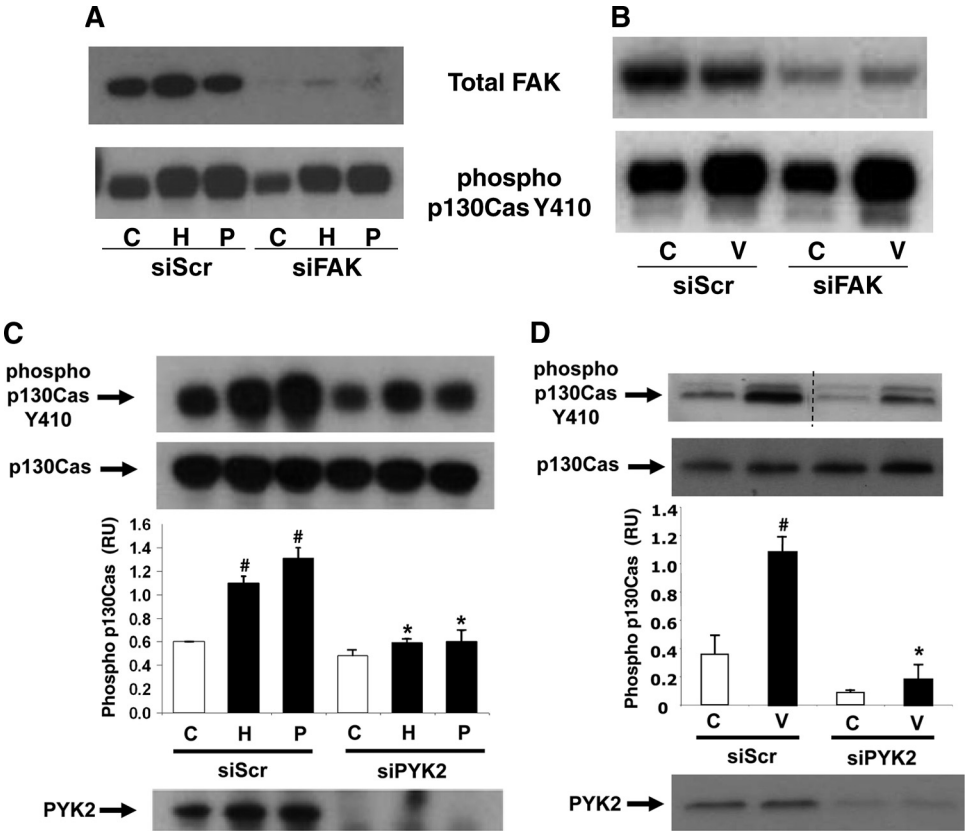

FIG. 4. Requirement of PYK2 for stimulation of $p130^{Cas}$ tyrosine phosphorylation. (A) U87MG cells were transfected with 25 nM siRNA targeting FAK (siFAK) or 25 nM siScr, and cells were treated as described in the legend to Fig. 1A. (B) HUVECs were transfected with 200 nM siFAK or 200 nM siScr, and cells were treated as described in the legend to Fig. 1B. (C) U87MG cells were transfected with 25 nM siRNA targeting PYK2 (siPYK2) or 25 nM siScr, and cells were treated as described in the legend to Fig. 1A. (D) HUVECs were transfected with 200 nM siPYK2 or 200 nM siScr, and cells were treated as described in the legend to Fig. 1B. Cell lysates were then prepared, blotted, and probed with the indicated antibodies. In panels C and D, $p130^{Cas}$ phosphorylation was quantified as described in the legend to Fig. 1. *, $P < 0.01$ (compared to siScr); #, $P < 0.05$ (compared to the control [C]). All of the samples in each film were run in the same gel, and blots were performed on the same membrane; samples on either side of the dashed lines in panel D were not adjacent but separated by lanes that were removed using computer software.

addition, treatment of HUVECs with either an NRP1-blocking antibody or a peptide antagonist, both of which inhibit VEGF binding to NRP1, also inhibited tyrosine phosphorylation of $p130^{Cas}$ (Fig. 1C). In addition, inhibition of $p130^{Cas}$ tyrosine phosphorylation by NRP1 knockdown was selective, since growth factor-mediated phosphorylation of ERK and AKT, two signaling molecules with well-established roles in regulating cell migration, was unaffected by treatment with NRP1 siRNA (Fig. 1D and E).

We next examined whether the NRP1 intracellular domain is required for growth factor stimulation of $p130^{Cas}$ tyrosine phosphorylation. To address this question, we generated Ad expressing either WT NRP1 (Ad.NRP1) or NRP1 lacking the entire C-terminal intracellular domain (Ad.NRP1ΔC) and used them to infect both U87MG cells and HUVECs. As shown in Fig. 2A and B, expression of Ad.NRP1ΔC decreased induction of $p130^{Cas}$ tyrosine phosphorylation in response to VEGF, HGF, and PDGF. Overexpression of Ad.NRP1 also resulted in some attenuation of VEGF-induced $p130^{Cas}$ phosphorylation in HUVECs, but the effect of Ad.NRP1ΔC was much greater (Fig. 2B). Using immunofluorescence microscopy, we could detect Ad.NRP1ΔC expression on the cell membrane, indicating that the effect of this mutant was unlikely to be due to incorrect processing or mislocalization (data not shown).

These findings raised the possibility that NRP1 may function by mediating RTK phosphorylation and activation. Previous studies indicate that in endothelial cells, NRP1 is required for optimal VEGFR2 phosphorylation (12, 18), and HGF receptor (c-Met) phosphorylation has been shown to be partially dependent on NRP1 expression (30). NRP1 knockdown caused a significant but partial decrease in VEGF-induced VEGFR2 tyrosine 1175 phosphorylation in HUVECs (Fig. 3A), while in U87MG cells, we found no difference in the level of either PDGFRβ or c-Met tyrosine phosphorylation between control and NRP1 siRNA-treated cells (Fig. 3B and C). One explanation for these results is that in endothelial cells, NRP1 might mediate $p130^{Cas}$ tyrosine phosphorylation at least in part through regulation of VEGFR2 tyrosine phosphorylation. However, this does not account for NRP1-dependent $p130^{Cas}$ tyrosine phosphorylation in response to HGF and PDGF. An alternative explanation is that NRP1 mediates a specific $p130^{Cas}$ signaling pathway which is dependent on its intracellular domain. To address this, we looked at the levels of RTK

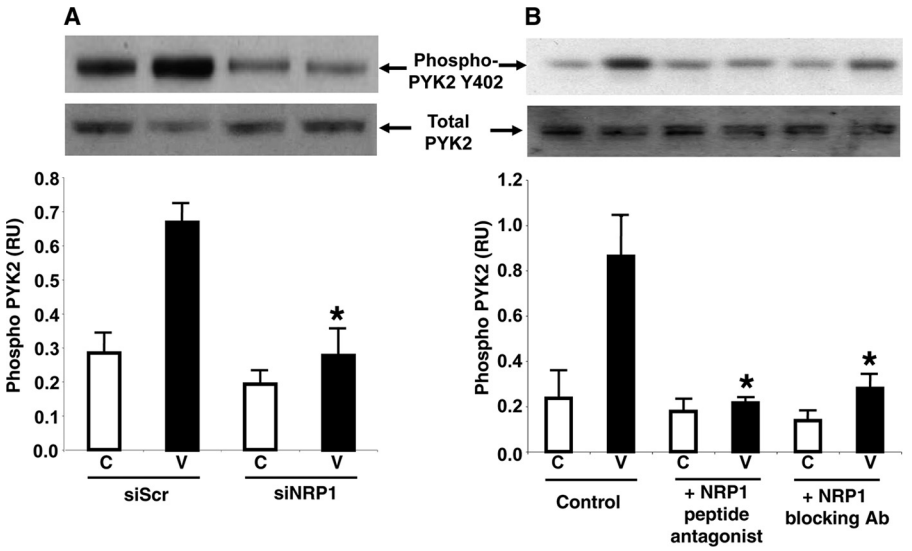

FIG. 5. VEGF-mediated tyrosine phosphorylation of PYK2 is dependent on NRP1 expression and the ability to bind VEGF. (A) HUVECs were transfected with 200 nM siNRP1 or 200 nM siScr and then treated as described in the legend to Fig. 1B. (B) Confluent HUVECs were preincubated for 30 min with 100 μM EG00086 (peptide antagonist), 5 μg/ml NRP1 blocking antibody (Ab), or the vehicle (water, control) and then stimulated ± 25 ng/ml VEGF for 10 min. Cell lysates were then prepared, blotted, and probed with the indicated antibodies. PYK2 phosphorylation was quantified as described in the legend to Fig. 1 and normalized to the total PYK2 level. *, $P < 0.05$ (compared to siScr and the control).

tyrosine phosphorylation in sample lysates from Fig. 2. As shown in Fig. 3D to F, the expression of neither Ad.NRP1 nor Ad.NRP1ΔC had any significant effect on ligand-stimulated phosphorylation of VEGFR2, c-Met, or PDGFRβ. These results provide direct evidence that the NRP1 intracellular domain is required for a specific signaling event downstream and independent of RTK activation.

In addition, we examined the role of synectin in growth factor-mediated p130Cas tyrosine phosphorylation. Synectin has been implicated in NRP1-mediated migration in response to EGF in endothelial cells overexpressing a chimeric EGF-NRP1 receptor (34), but analysis of synectin-deficient mice showed that growth factor-stimulated migration of venous endothelial cells was not impaired (4). Treatment of both U87MG cells and HUVECs with siRNA to synectin markedly reduced synectin expression but had no effect on growth factor-induced tyrosine phosphorylation of p130Cas (data not shown). Our results suggest the involvement of an unidentified NRP1-associating protein(s) required for signaling to p130Cas, a possibility that warrants further work.

Although Src directly phosphorylates p130Cas at focal adhesions within a macromolecular complex requiring focal adhesion kinase (FAK) (5, 26), we detected no changes in the level of tyrosine phosphorylation of Src or FAK in U87MG cells

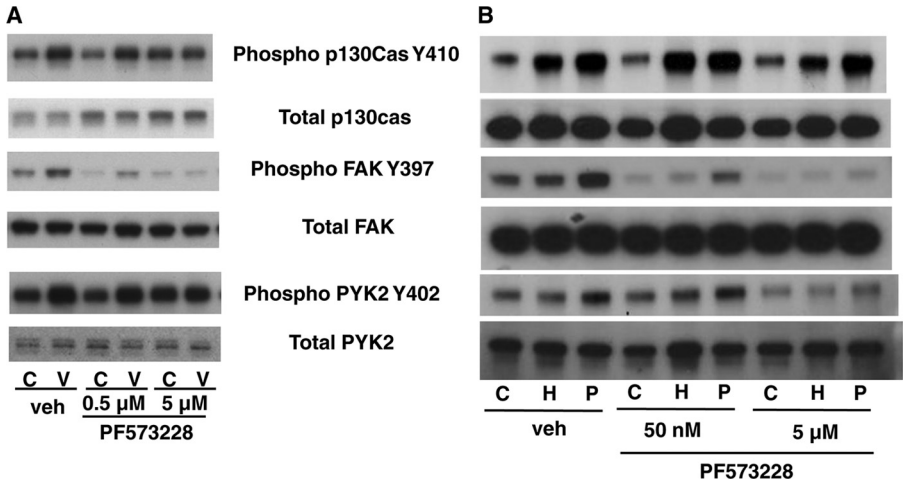

FIG. 6. FAK inhibition does not affect growth factor stimulation of p130Cas phosphorylation. (A) Confluent HUVECs were preincubated for 30 min with 0.5 or 5 μM PF573228 or the vehicle (0.05% [vol/vol] DMSO) (veh). Cells were then treated as described in the legend to Fig. 1B. (B) U87MG cells were pretreated for 30 min with the vehicle alone or with PF573228 at 50 nM or 5 μM. Cells were then treated as described in the legend to Fig. 1A. Cell lysates were then prepared, blotted, and probed with the indicated antibodies. The blots shown are representative of at least three independent experiments.

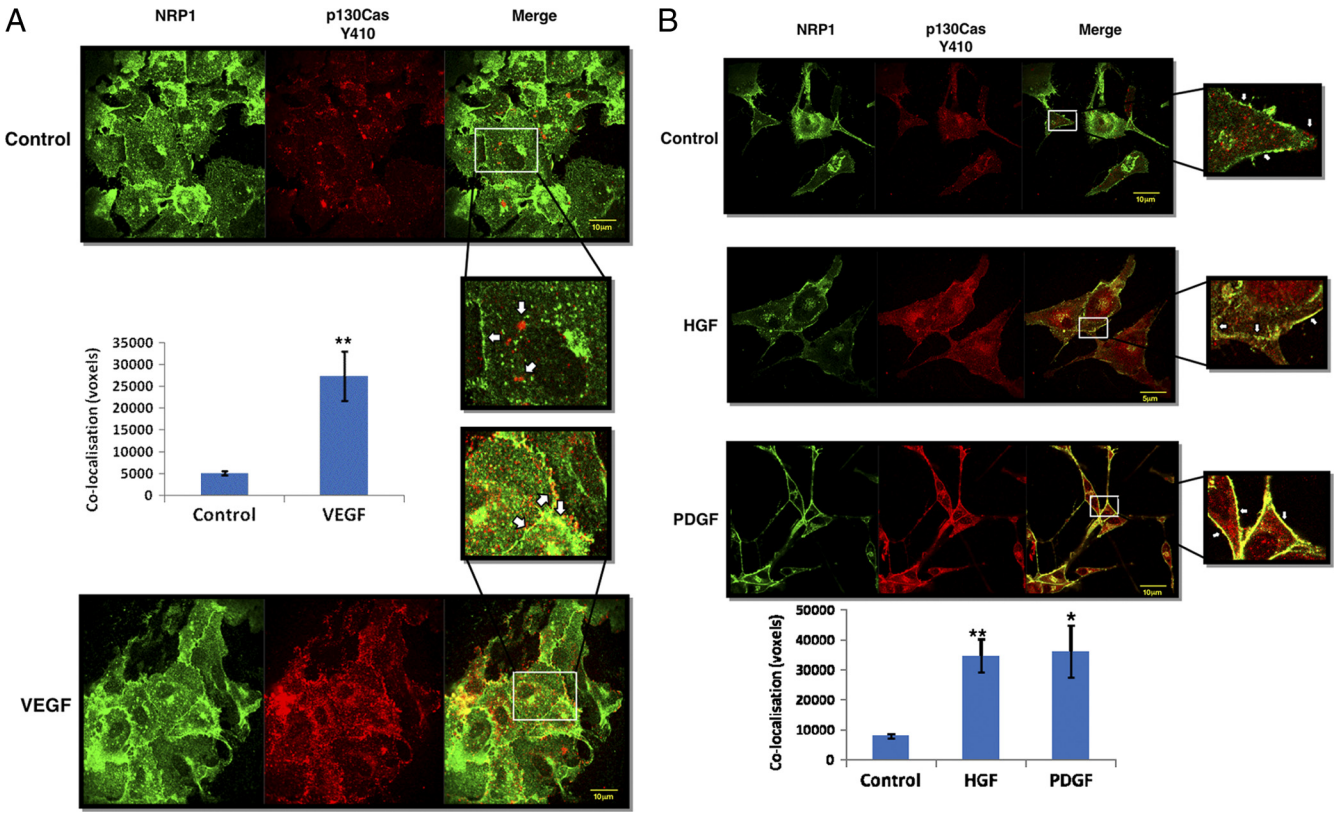

FIG. 7. Growth factor-mediated increase in colocalization of NRP1 and tyrosine-phosphorylated p130^{Cas}. (A) HUVECs were seeded onto glass coverslips and incubated in 0.5% FCS in EBM for ~18 h prior to treatment with the SFM vehicle control or with 25 ng/ml VEGF. (B) U87MG cells were seeded onto glass coverslips and incubated in SFM for ~18 h prior to treatment with the SFM vehicle control or with 25 ng/ml HGF or 50 ng/ml PDGF-BB for 5 min. Confocal imaging was performed as described in Materials and Methods, with NRP1 staining in green and phospho-p130^{Cas} (Y410) staining in red. Merged images show costaining of NRP1 and phospho-p130^{Cas} Y410 in yellow and are representative of at least three separate experiments. Quantification of NRP1 and phospho-p130^{Cas} colocalization (as described in Materials and Methods) is shown in the graphs and represents data from three independent experiments expressed as colocalization in the number of voxels (means ± SEM). *, $P < 0.05$ (compared to the SFM control).

expressing S612A NRP1 (9). Furthermore, NRP1 siRNA had no effect on growth factor-stimulated FAK autophosphorylation (Y397) (data not shown), and FAK siRNA treatment had no effect on ligand-stimulated p130^{Cas} tyrosine phosphorylation (Fig. 4A and B). A recent report showed that the FAK-related kinase PYK2 mediates endothelin-1 signaling via p130^{Cas} (23), and therefore we investigated whether PYK2 is required for growth factor-induced p130^{Cas} phosphorylation. siRNA knockdown of PYK2 in U87MG cells and HUVECs strongly inhibited p130^{Cas} phosphorylation induced by HGF, PDGF, and VEGF (Fig. 4C and D). Furthermore, either inhibition of VEGF binding to NRP1 or NRP1 knockdown in HUVECs reduced VEGF-induced PYK2 tyrosine phosphorylation (Fig. 5A and B). In contrast, treatment of U87MG cells with NRP1 siRNA had no effect on PYK2 phosphorylation (data not shown). Pharmacological inhibition with the potent FAK family inhibitor PF573228 at concentrations which specifically block FAK kinase activity (27) had no effect on ligand-stimulated p130^{Cas} tyrosine phosphorylation (Fig. 6A and B). However, when we used PF573228 at a concentration which inhibits both FAK and PYK2 activities (27), we detected a dramatic decrease in VEGF-mediated p130^{Cas} tyrosine phosphorylation, while we saw no effect on the response to HGF and PDGF in U87MG cells (Fig. 6A and B). These results suggest that PYK2 is an upstream kinase required for VEGF-induced tyrosine phosphorylation of p130^{Cas}. In contrast, although PYK2 expression is important for HGF- and PDGF-induced p130^{Cas} tyrosine phosphorylation, PYK2 activity is not. Therefore, NRP1 signaling to p130^{Cas} is most likely mediated through another tyrosine kinase in U87MG cells.

Recent reports have described tyrosine-phosphorylated p130^{Cas} as being present in focal adhesion complexes, whereas NRP1 is present predominantly at the plasma membrane and in cytosolic vesicles (6, 9). Using immunofluorescence confocal microscopy, we examined the distribution of NRP1 and tyrosine-phosphorylated p130^{Cas} in both HUVECs and U87MG cells. Under basal, unstimulated conditions, tyrosine-phosphorylated p130^{Cas} was localized in focal adhesions with little staining evident at the plasma membrane, whereas NRP1 was present at the plasma membrane and in the cytosol but absent from focal adhesion-like structures (Fig. 7A and B). In both HUVECs and U87MG cells, growth factor stimulation resulted in a large increase in the colocalization of NRP1 with tyrosine-phosphorylated p130^{Cas} at the plasma membrane (Fig. 7A and B). These data further support the role of NRP1 as an important mediator of signaling via p130^{Cas} tyrosine

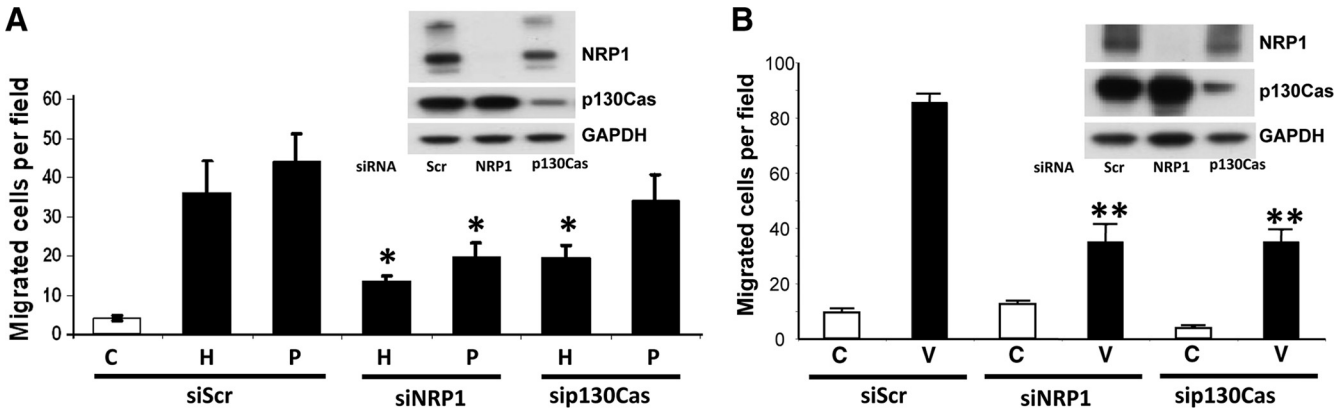

FIG. 8. Requirement of NRP1 and p130Cas for HGF, PDGF, and VEGF stimulation of chemotactic migration of U87MG cells and HUVECs. (A) U87MG cells were transfected with 25 nM siNRP1, 25 nM sip130Cas, or 25 nM siScr for 48 h. Cell migration in response to 25 ng/ml HGF or 50 ng/ml PDGF-BB was then determined in a Transwell migration assay as described in Materials and Methods. (B) HUVECs were transfected with 200 nM siNRP1, 200 nM sip130Cas, or 200 nM siScr for 48 h, and cell migration in response to 25 ng/ml VEGF-A was determined as described for panel A. Values ($n \geq 3$) are means ± SEM, expressed as the number of cells migrating per field; *, $P < 0.05$; **, $P < 0.01$ (compared to siScr). Insets show representative blots of siRNA-mediated knockdown of NRP1 and p130Cas.

phosphorylation, which involves growth factor-stimulated recruitment of p130Cas to the plasma membrane, where it colocalizes with NRP1. p130Cas is reported to associate with PYK2 and FAK (5, 23), and we confirmed that p130Cas forms complexes with these kinases in HUVECs and U87MG cells, as demonstrated by coimmunoprecipitation, but p130Cas coimmunoprecipitation with PYK2 and FAK was not affected by growth factor stimulation or NRP1 siRNA (data not shown). Furthermore, we were unable to coimmunoprecipitate NRP1 with p130Cas, FAK, or PYK2, though this may simply reflect a weak or transient interaction or possibly limitations of our reagents in coimmunoprecipitation assays. Although the exact nature of a constitutive PYK2-p130Cas-FAK complex is unclear, our results point to a critical role for PYK2 in the tyrosine phosphorylation of p130Cas. In endothelial cells, PYK2 kinase activity is upstream of p130Cas, while in U87MG cells, PYK2 may act as a scaffold for the recruitment of other signaling molecules necessary for p130Cas tyrosine phosphorylation.

Though p130Cas has been implicated in signaling required for cell motility, little is known about the role of p130Cas either in endothelial cell migration stimulated by VEGF or in tumor cell migration in response to HGF and PDGF. We therefore examined ligand-mediated chemotactic migration in both U87MG cells and HUVECs. Knockdown of p130Cas expression in U87MG cells and HUVECs using siRNA significantly reduced HGF- and VEGF-mediated chemotactic migration, respectively. In addition, both U87MG cells and HUVECs treated with siRNA to NRP1 exhibited a significant reduction in ligand-stimulated chemotactic migration (Fig. 8A and B). Surprisingly, p130Cas knockdown did not significantly reduce PDGF-mediated migration of U87MG cells. We hypothesized that PDGF is capable of promoting migration in the absence of p130Cas due to the mesenchymal-to-amoeboid transition observed in invading U87MG cells upon p130Cas silencing as we previously reported (9). It is well established that many human tumor cells have the capacity to switch their mode of motility when challenged by changes in their intracellular or extracellular environment (24). Although most studies on tumor cell plasticity have been performed using three-dimensional matrices, human neutrophils, which exhibit an amoeboid mode of motility (32), are capable of migrating in two dimensions along a PDGF-mediated chemotactic gradient (31). As shown in Fig. 9A, we confirmed with the use of an additional siRNA that p130Cas silencing leads to a dramatic mesenchymal-to-amoeboid transition of U87MG cells when adhering to tissue culture plastic. In contrast, we did not observe a morphological change in HUVECs treated with p130Cas siRNA (Fig. 9B), indicating that HUVECs do not possess the same morphological plasticity. Interestingly, as described above, HGF-mediated migration was significantly reduced in amoeboid U87MG cells, indicating that HGF is insufficient to mediate chemotaxis using this mode of motility in these cells. Indeed, there is a recent report showing that HGF treatment induces the opposite, an amoeboid-to-mesenchymal transition of two-dimensionally migrating HeLa cells (17). Furthermore, in agreement with the results of our migration studies (Fig. 8A), treatment of U87MG cells with NRP1 siRNA did not cause a mesenchymal-to-amoeboid transition (Fig. 9A).

Given these observations, we evaluated the role of p130Cas tyrosine phosphorylation in mediating growth factor-induced chemotactic migration by Ad expression of WT p130Cas (Ad.p130Cas) or a mutant form of p130Cas (Ad.p130Cas15F) containing Y/F mutations in all 15 YXXP consensus motifs within the p130Cas SD. These YXXP motifs represent potential SH2 domain binding sites, and previous studies have shown that complete deletion of the p130Cas SD inhibits the assembly of docking proteins, leading to loss of cell migration (14). Furthermore, a recent report showed that expression of the p130Cas15F mutant form in human pancreatic tumor cells led to a decrease in EGF-mediated p130Cas tyrosine phosphorylation and cell migration (21). Expression of either Ad.p130Cas or Ad.p130Cas15F in U87MG cells did not result in a mesenchymal-to-amoeboid transition in cell morphology (Fig. 9C). Infection of U87MG cells and HUVECs with Ad.p130Cas15F markedly reduced HGF, PDGF, and VEGF stimulation of

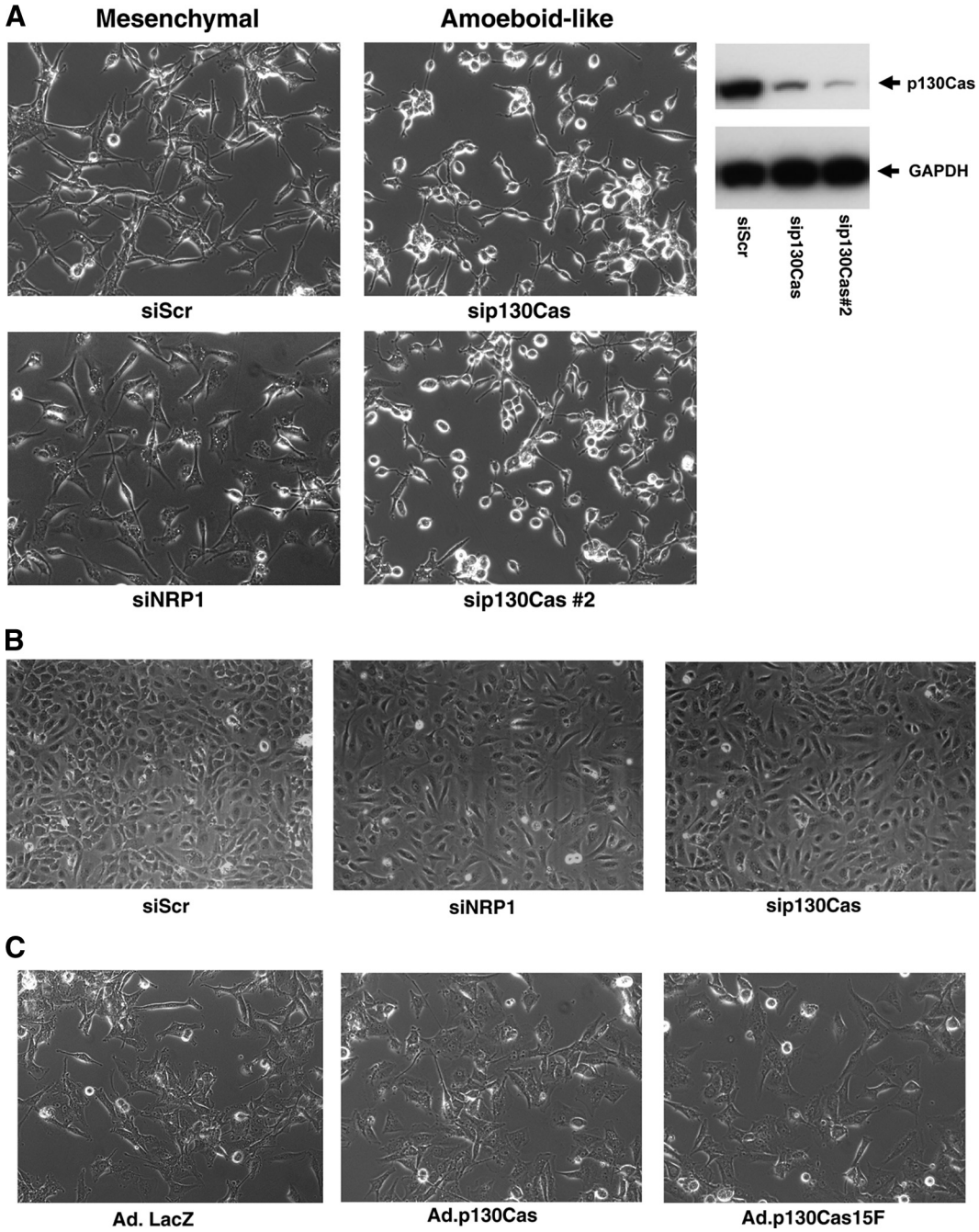

FIG. 9. p130^{Cas} regulates U87MG cell plasticity. (A) U87MG cells were transfected with 25 nM sip130^{Cas}, 25 nM sip130^{Cas}#2, or 25 nM siScr for 48 h. Cells were incubated for 18 h in SFM, and pictures were obtained using a Zeiss Axiovert 200 inverted microscope. The inset shows levels of p130^{Cas} knockdown. (B) HUVECs were transfected with 200 nM sip130^{Cas} or 200 nM siScr for 48 h. Cells were incubated for 18 h in 0.5% (vol/vol) serum, and pictures were obtained as described for panel A. (C) U87MG cells were infected with Ad.LacZ, Ad.p130^{Cas}, or Ad.p130^{Cas15F}. At 48 h after infection, cells were incubated in SFM for ~18 h and pictures were obtained as before.

p130^{Cas} tyrosine phosphorylation, indicating a dominant negative effect of the p130^{Cas15F} protein (Fig. 10A and B). Interestingly, expression of Ad.p130^{Cas} in HUVECs led to an increase in basal and VEGF-induced tyrosine phosphorylation, which was not observed in U87MG cells (Fig. 10A and B). In agreement with an important role for p130^{Cas} tyrosine phosphorylation in chemotactic migration, expression of Ad.p130^{Cas15F} significantly reduced growth factor-mediated migration in both cell types (Fig. 10C and D). Furthermore, expression of Ad.p130^{Cas} had no effect on migration, indicating that p130^{Cas} tyrosine phosphorylation is necessary but not sufficient for migration. These results show that p130^{Cas} tyrosine phosphorylation is required for mediating chemotactic migration and point to an important role for p130^{Cas} in maintaining

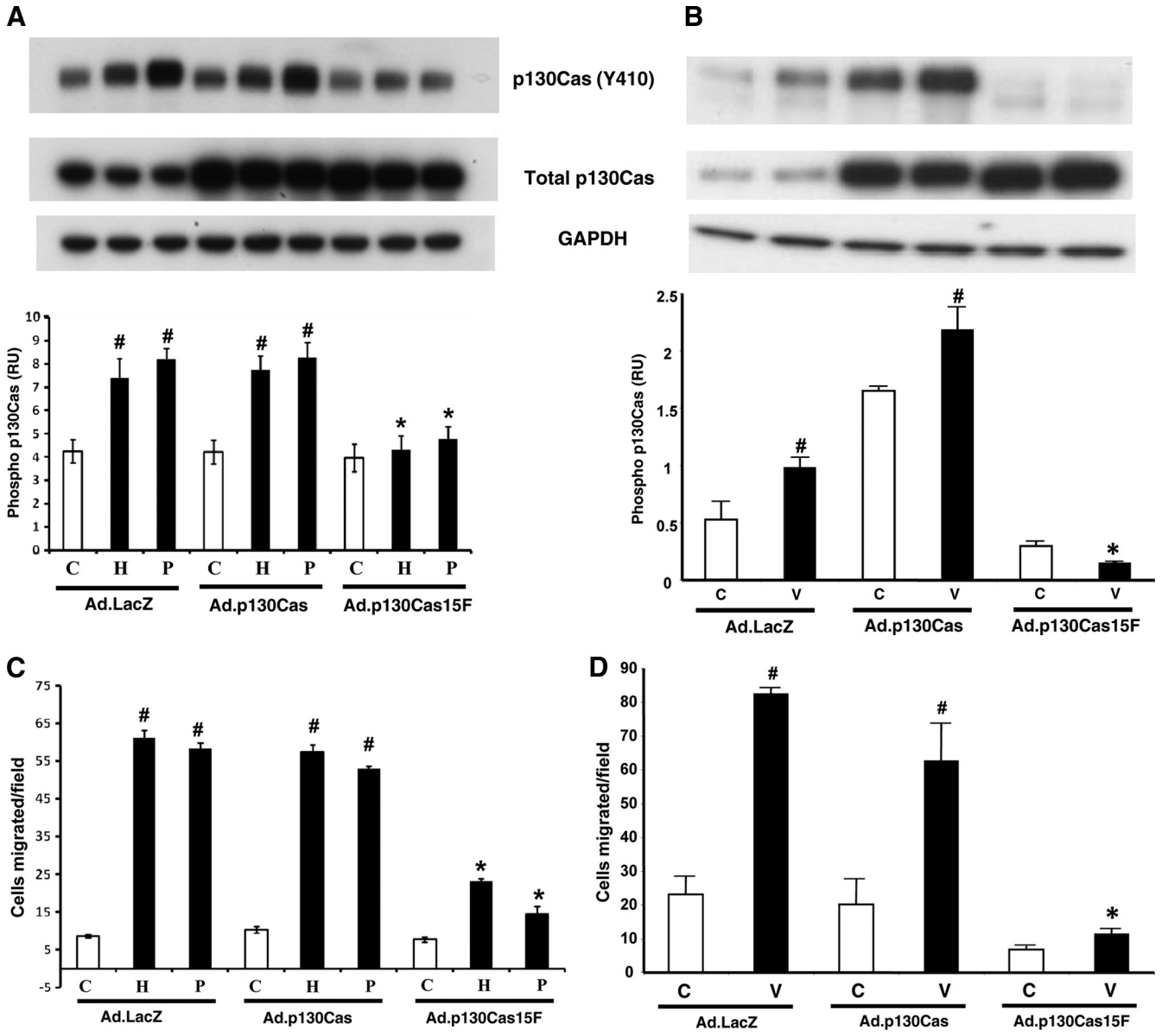

FIG. 10. $p130^{Cas}$ tyrosine phosphorylation is required for chemotactic migration of U87MG cells and HUVECs. (A and B) U87MG cells and HUVECs were infected with Ad.LacZ, Ad.$p130^{Cas}$, and Ad.$p130^{Cas15F}$ and treated 48 h later with HGF, PDGF, and VEGF as described in the legend to Fig. 2. Data from three independent experiments are presented as relative units (RU) of $p130^{Cas}$ phosphorylation (means ± SEM) normalized to GAPDH. *, $P < 0.01$ (compared to Ad.$p130^{Cas}$ plus growth factor); #, $P < 0.01$ (compared to the control [C]). (C and D) Cells were infected as described for panels A and B, and 48 h later, migration stimulated by HGF and PDGF in U87MG cells and by VEGF in HUVECs was assayed as described in the legend to Fig. 8. Values ($n \geq 3$) are means ± SEM, expressed as the number of cells migrating per field. *, $P < 0.01$ (compared to Ad.$p130^{Cas}$ plus growth factor); #, $P < 0.01$ (compared to the control [C]).

the mesenchymal morphology of U87MG cells, which may be dependent on protein expression and/or basal phosphorylation.

We next examined the role of the NRP1 intracellular domain in growth factor-mediated chemotactic migration. Ad.NRP1ΔC expression in U87MG cells significantly inhibited migration induced by either HGF or PDGF (Fig. 11A). Similarly, in HUVECs, VEGF-induced chemotactic migration was strongly inhibited by the expression of Ad.NRP1ΔC, whereas Ad.NRP1 had no significant effect on endothelial cell migration compared to the control, Ad.GFP (Fig. 11B). It is interesting that in HUVECs, expression of Ad.NRP1ΔC caused a greater reduction of VEGF-stimulated migration than treatment with NRP1 siRNA. This most probably results from a dominant negative effect of Ad.NRP1ΔC resulting from the sequestration of NRP1, NRP2, and VEGFR2 in nonfunctional complexes. These results are consistent with the inhibitory effects of Ad.NRP1ΔC on $p130^{Cas}$ tyrosine phosphorylation (Fig. 2A and B) and further establish the role of the NRP1 intracellular domain in regulating RTK-mediated signaling and migration.

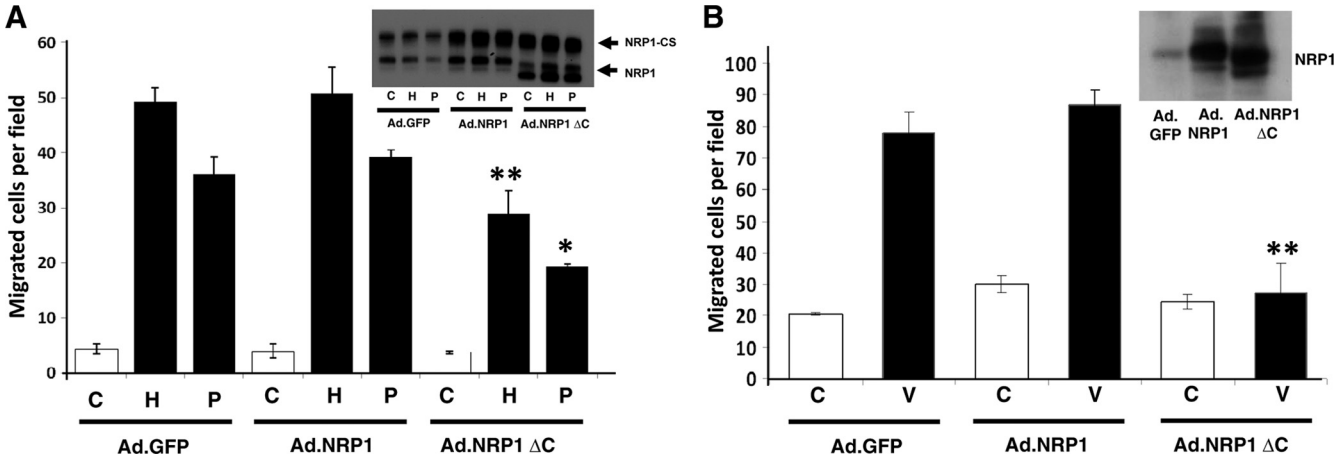

FIG. 11. Requirement of NRP1 intracellular domain for HGF, PDGF, and VEGF stimulation of chemotactic migration of U87MG cells and HUVECs. (A) U87MG cells were infected with Ad.GFP, Ad.NRP1, or Ad.NRP1ΔC for 48 h. Cell migration in response to 25 ng/ml HGF or 50 ng/ml PDGF was then determined. (B) Confluent HUVECs were infected with Ad.GFP, Ad.NRP1, or Ad.NRP1ΔC for 48 h, and cell migration in response to 25 ng/ml VEGF was determined. The inset shows levels of NRP1 and NRP1ΔC expression. Values ($n \geq 3$) are means ± SEM, expressed as the number of cells migrating per field. *, $P < 0.05$; **, $P < 0.01$ (compared to Ad.NRP1 plus growth factor).

In addition to VEGF signaling through NRP1/VEGFR2 receptor complexes in endothelial cells, NRP1 has been reported to associate with the c-Met receptor and HGF has been reported to be an NRP1 ligand in tumor cells (15, 30). Similarly, tumor cell-derived PDGF has been reported to be a ligand for NRP1 expressed on smooth muscle cells (2). However, these studies are based on coimmunoprecipitation experiments and lack data on binding kinetics and affinity. We were unable to observe any association between NRP1 and either c-Met or PDGFRβ (data not shown). The role of NRP1 in regulating RTK signaling in various cell types is still emerging, and the specific pathways involved have yet to be fully elucidated. We do, however, find that NRP1 has a specific role in regulating RTK-mediated tyrosine phosphorylation of $p130^{Cas}$, since NRP1 knockdown did not significantly affect other major RTK signal transduction pathways (Fig. 1D and E). Furthermore, our results indicate that VEGF binding to NRP1 mediates VEGFR2 phosphorylation (Fig. 3A) and is critical for tyrosine phosphorylation of $p130^{Cas}$ (Fig. 1C). Therefore, in endothelial cells, NRP1 plays a dual role in both regulation of VEGFR2 phosphorylation and $p130^{Cas}$ phosphorylation. Ligand stimulation of $p130^{Cas}$ tyrosine phosphorylation requires expression of RTKs, because knockdown of VEGFR2 in HUVECs and c-Met in U87MG cells inhibited $p130^{Cas}$ tyrosine phosphorylation (data not shown). Since NRP1 knockdown reduced VEGFR2 phosphorylation at Y1175 by ~50% (Fig. 3A), it is plausible that the differential effect of NRP1 knockdown on VEGF-stimulated $p130^{Cas}$ phosphorylation compared with other VEGFR2-mediated signaling pathways is a consequence of $p130^{Cas}$ tyrosine phosphorylation requiring a higher level of VEGFR2 activation. In contrast, ERK and AKT activation is unaffected by attenuation of VEGFR2 activity since they may have a lower threshold receptor activity. Given that the NRP1 intracellular domain is important for RTK signaling through $p130^{Cas}$, we propose that NRP1 participates in protein-protein interactions which result in activation and/or recruitment of specific signaling components, including $p130^{Cas}$ and PYK2, to an NRP1/RTK complex.

This is the first study clearly establishing a role for NRP1 in a specific cell signaling pathway. Moreover, the finding that growth factor stimulation of $p130^{Cas}$ tyrosine phosphorylation requires the NRP1 intracellular domain strongly suggests that this region directly mediates intracellular signaling leading to $p130^{Cas}$ tyrosine phosphorylation, presumably through protein-protein interactions with an as-yet-unidentified cytosolic binding partner. In addition, we have shown that PYK2 expression is required for $p130^{Cas}$ tyrosine phosphorylation in response to PDGF, HGF, and VEGF and that in endothelial cells, PYK2 phosphorylation is dependent upon NRP1. Together, these results indicate that NRP1 regulates endothelial and tumor cell chemotactic migration through a novel $p130^{Cas}$ pathway, which has implications for the mechanisms involved in angiogenesis and tumor metastasis.

ACKNOWLEDGMENTS

This work was supported by British Heart Foundation grants FS/06/019 to C.P.-M. and RG/06/003 to I.E., M.Y., G.B., and I.Z. and by funding from Ark Therapeutics Limited.

We thank David Selwood, Haiyan Jia, and Ashley Jarvis for the synthesis and characterization of EG00086.

REFERENCES

1. **Avraham, H. K., et al.** 2003. Vascular endothelial growth factor regulates focal adhesion assembly in human brain microvascular endothelial cells through activation of the focal adhesion kinase and related adhesion focal tyrosine kinase. J. Biol. Chem. **278:**36661–36668.
2. **Banerjee, S., et al.** 2006. Breast cancer cells secreted platelet-derived growth factor-induced motility of vascular smooth muscle cells is mediated through neuropilin-1. Mol. Carcinog. **45:**871–880.
3. **Cai, H., and R. R. Reed.** 1999. Cloning and characterization of neuropilin-1-interacting protein: a PSD-95/Dlg/ZO-1 domain-containing protein that interacts with the cytoplasmic domain of neuropilin-1. J. Neurosci. **19:**6519–6527.
4. **Chittenden, T. W., et al.** 2006. Selective regulation of arterial branching morphogenesis by synectin. Dev. Cell **10:**783–795.
5. **Defilippi, P., P. Di Stefano, and S. Cabodi.** 2006. $p130^{Cas}$: a versatile scaffold in signaling networks. Trends Cell Biol. **16:**257–263.
6. **Donato, D. M., L. M. Ryzhova, L. M. Meenderink, I. Kaverina, and S. K. Hanks.** 2010. Dynamics and mechanism of $p130^{Cas}$ localization to focal adhesions. J. Biol. Chem. **285:**20769–20779.
7. **Endo, A., S. Fukuhara, M. Masuda, T. Ohmori, and N. Mochizuki.** 2003. Selective inhibition of vascular endothelial growth factor receptor-2

(VEGFR-2) identifies a central role for VEGFR-2 in human aortic endothelial cell responses to VEGF. J. Recept. Signal Transduct. Res. **23:**239–254.
8. **Evans, I. M., G. Britton, and I. C. Zachary.** 2008. Vascular endothelial growth factor induces heat shock protein (HSP) 27 serine 82 phosphorylation and endothelial tubulogenesis via protein kinase D and independent of p38 kinase. Cell Signal. **20:**1375–1384.
9. **Frankel, P., et al.** 2008. Chondroitin sulphate-modified neuropilin 1 is expressed in human tumour cells and modulates 3D invasion in the U87MG human glioblastoma cell line through a p130^{Cas}-mediated pathway. EMBO Rep. **9:**983–989.
10. **Gu, C., et al.** 2003. Neuropilin-1 conveys semaphorin and VEGF signaling during neural and cardiovascular development. Dev. Cell **5:**45–57.
11. **Hu, B., et al.** 2007. Neuropilin-1 promotes human glioma progression through potentiating the activity of the HGF/SF autocrine pathway. Oncogene **26:**5577–5586.
12. **Jia, H., et al.** 2006. Characterization of a bicyclic peptide neuropilin-1 (NP-1) antagonist (EG3287) reveals importance of vascular endothelial growth factor exon 8 for NP-1 binding and role of NP-1 in KDR signaling. J. Biol. Chem. **281:**13493–13502.
13. **Jia, H., et al.** 2008. N-capped peptides with NP-1 antagonist activity. U.S. patent WO/2008/040978.
14. **Klemke, R. L., et al.** 1998. CAS/Crk coupling serves as a "molecular switch" for induction of cell migration. J. Cell Biol. **140:**961–972.
15. **Matsushita, A., T. Gotze, and M. Korc.** 2007. Hepatocyte growth factor-mediated cell invasion in pancreatic cancer cells is dependent on neuropilin-1. Cancer Res. **67:**10309–10316.
16. **Oh, H., et al.** 2002. Selective induction of neuropilin-1 by vascular endothelial growth factor (VEGF): a mechanism contributing to VEGF-induced angiogenesis. Proc. Natl. Acad. Sci. U. S. A. **99:**383–388.
17. **Palamidessi, A., et al.** 2008. Endocytic trafficking of Rac is required for the spatial restriction of signaling in cell migration. Cell **134:**135–147.
18. **Pan, Q., et al.** 2007. Blocking neuropilin-1 function has an additive effect with anti-VEGF to inhibit tumor growth. Cancer Cell **11:**53–67.
19. **Pellet-Many, C., P. Frankel, H. Jia, and I. Zachary.** 2008. Neuropilins: structure, function and role in disease. Biochem. J. **411:**211–226.
20. **Prahst, C., et al.** 2008. Neuropilin-1-VEGFR-2 complexing requires the PDZ-binding domain of neuropilin-1. J. Biol. Chem. **283:**25110–25114.
21. **Ricono, J. M., et al.** 2009. Specific cross-talk between epidermal growth factor receptor and integrin alphavbeta5 promotes carcinoma cell invasion and metastasis. Cancer Res. **69:**1383–1391.
22. **Rivera, G. M., et al.** 2006. Requirement of Nck adaptors for actin dynamics and cell migration stimulated by platelet-derived growth factor B. Proc. Natl. Acad. Sci. U. S. A. **103:**9536–9541.
23. **Rufanova, V. A., A. Alexanian, T. Wakatsuki, A. Lerner, and A. Sorokin.** 2009. Pyk2 mediates endothelin-1 signaling via p130^{Cas}/BCAR3 cascade and regulates human glomerular mesangial cell adhesion and spreading. J. Cell. Physiol. **219:**45–56.
24. **Sahai, E.** 2005. Mechanisms of cancer cell invasion. Curr. Opin. Genet. Dev. **15:**87–96.
25. **Salikhova, A., et al.** 2008. Vascular endothelial growth factor and semaphorin induce neuropilin-1 endocytosis via separate pathways. Circ. Res. **103:**e71–e79.
26. **Sharma, A., and B. J. Mayer.** 2008. Phosphorylation of p130^{Cas} initiates Rac activation and membrane ruffling. BMC Cell Biol. **9:**50.
27. **Slack-Davis, J. K., et al.** 2007. Cellular characterization of a novel focal adhesion kinase inhibitor. J. Biol. Chem. **282:**14845–14852.
28. **Soker, S., H. Q. Miao, M. Nomi, S. Takashima, and M. Klagsbrun.** 2002. VEGF165 mediates formation of complexes containing VEGFR-2 and neuropilin-1 that enhance VEGF165-receptor binding. J. Cell. Biochem. **85:**357–368.
29. **Soker, S., S. Takashima, H. Q. Miao, G. Neufeld, and M. Klagsbrun.** 1998. Neuropilin-1 is expressed by endothelial and tumor cells as an isoform-specific receptor for vascular endothelial growth factor. Cell **92:**735–745.
30. **Sulpice, E., et al.** 2008. Neuropilin-1 and neuropilin-2 act as coreceptors, potentiating proangiogenic activity. Blood **111:**2036–2045.
31. **Thelen, M., M. Uguccioni, and J. Bosiger.** 1995. PI 3-kinase-dependent and independent chemotaxis of human neutrophil leukocytes. Biochem. Biophys. Res. Commun. **217:**1255–1262.
32. **Valerius, N. H., O. Stendahl, J. H. Hartwig, and T. P. Stossel.** 1981. Distribution of actin-binding protein and myosin in polymorphonuclear leukocytes during locomotion and phagocytosis. Cell **24:**195–202.
33. **Wang, L., D. Mukhopadhyay, and X. Xu.** 2006. C terminus of RGS-GAIP-interacting protein conveys neuropilin-1-mediated signaling during angiogenesis. FASEB J. **20:**1513–1515.
34. **Wang, L., H. Zeng, P. Wang, S. Soker, and D. Mukhopadhyay.** 2003. Neuropilin-1-mediated vascular permeability factor/vascular endothelial growth factor-dependent endothelial cell migration. J. Biol. Chem. **278:**48848–48860.
35. **Whitaker, G. B., B. J. Limberg, and J. S. Rosenbaum.** 2001. Vascular endothelial growth factor receptor-2 and neuropilin-1 form a receptor complex that is responsible for the differential signaling potency of VEGF(165) and VEGF(121). J. Biol. Chem. **276:**25520–25531.